Schweizerische Eidgenossenschaft
Confédération suisse
Confederazione Svizzera
Confederaziun svizra

Federal Department of the Environment, Transport, Energy and Communications DETEC

Swiss Federal Office of Energy SFOE
Energy Research and Cleantech Division

REEL Demo – Romande Energie ELectric network in local balance Demonstrator

Deliverable: 5c Definition of optimal control of DWH for self-consumption strategies

Demo site: Rolle

Developed by
Jordan HOLWEGER (EPFL-PVlab)
Lionel BLOCH (EPFL-PVlab)
Nicolas WYRSCH (EPFL-PVlab)

[Neuchâtel, 27.12.2020]

Contents

Executive summary

The massive integration of renewable energy, and the electrification of the building heating systems are required in order to meet the Paris agreement's CO2 emission target. Heat pumps and PV is expected to penetrate quickly in the market come with significant investment costs. To maximize the profit and advantage of both technologies without increasing their management complexity, novel algorithms guaranteeing close-to-optimal operations should be demonstrated.

In this work, a novel heuristic control algorithm is presented. The algorithm optimizes an indicator comparing the variation of the operating cost and the generated heat. It is versatile and agnostic of the building modeling complexity. The benchmark against a mixed-integer linear formulation of the energy management shows that the proposed algorithm performs closely to the optimal solution. The differences in terms of operating costs and temperature deviations are negligible. The simplicity of the algorithm makes it suitable for implementing in a micro-controller as a state machine.

1 Description of the deliverable and goal

In the energy transition and the Swiss 2050 energy strategy framework, a high penetration of distributed photovoltaic (PV) systems is expected. This implies a shift from a centralized to a decentralized energy provision system. Furthermore, to cope with the Paris agreement's CO_2 emission target, the electrification of the building heating system is required (representing a large third of the final Swiss energy demand, see Figure 1). These two critical elements of the energy transition will have a substantial impact on our electrical grid and how modern energy systems are designed and operated.

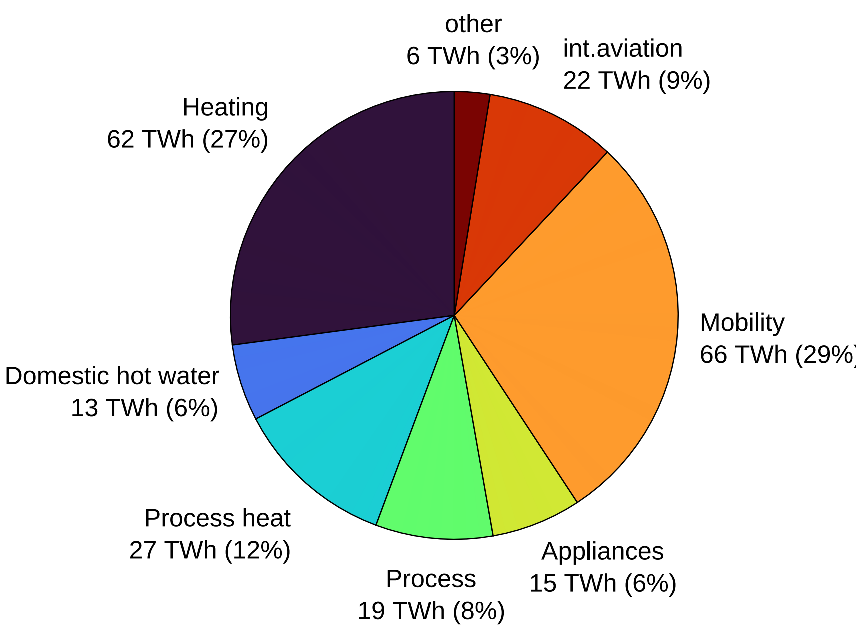

Figure 1: Final Swiss energy demand by application adapted from [1]. The appliances category gather Lightning, IT & Entertainment, ventilation & AC needs.

At the scale of an individual building, there is a growing need for technologies enabling optimal system operation by acting on controllable loads. The heating system (assuming converting electricity to heat) is typically a controllable load because the thermal inertia allows for load shifting with a low impact on the occupants' comfort. Using a heat pump (HP) is an obvious choice for the simple thermodynamic reason that one electricity unit fed to the device generates more than one heat unit. The question is how to control the HP so that it fulfills its duty of providing heat and maintain the occupants' comfort while leading to the minimum possible operating cost by using as much as possible of the cheap available PV energy?

This work aims to provide a simple and effective HP control algorithm for PV systems aiming to maximize such a system's profitability, hence reducing the operating cost. This work describes the formulation of a heuristic control strategy designed to be versatile in terms of modeling equation requirements, and lean in terms of computational resource requirements. The proposed algorithm is based on an indicator rather than a complex objective function, ensuring the computation's simpleness.

1.1 Research question

This work aims to answer the following research question:

- What is the optimal control trajectory of a HP to minimize the operating costs?
- Which algorithm can provide a HP control trajectory leading to an operating as close as possible to the optimal cost while being lean in terms of computation requirements and versatile in term of modelling complexity?

1.2 Novelty of the proposed solutions compared to the state-of-art

The building energy management problem has attracted a wide range of research aiming to address this problem from various perspectives or using different techniques. Regarding the thermal and electrical supply management, the first category is to use quadratic formulation to get the absolute optimal solution. For instance, mixed-integer linear programming (MILP) can be used as in [2, 3, 4, 5] to obtain the optimal size and operation of the component (HP, PV, battery, and thermal energy storage). This technique requires, however, linear or at least quadratic objective and constraint functions. The second practice is to use meta-heuristic optimization [6, 7, 8, 9]. Meta-heuristics typically focus on quickly getting a feasible (non-linear constraints are admissible) solution, but their optimality still needs to be demonstrated. The advantage of using such a technique is to allow any kind of non-linearities in the input model. The first two categories are focused on the formulation of an optimization problem and how to solve it. The energy management problem can also be tackled from a control perspective.

Model predictive control is a well-known approach extensively used to solve the energy management problem [10, 11, 12]. This technique can be extended using dynamic optimization like in [13]. This approach suffers from an extended complexity inherent to the fact that very accurate models are usually used and that the definition of the objective function is not so straight forward. The influence of the objective function's formulation (despite aiming to the same conceptual goal) can indeed widely change the resulting operation [6]. For instance, instead of using the comfort temperature as hard bounds (often used in MILP approaches), a comfort penalty is integrated into the objective function [14]. The difficulty with such a method of combining heterogeneous metrics in the objective function is to find the appropriate weights so that the solution is a good trade-off between the various objectives.

The final approach for the HP control is to use a heuristic approach similar to [15, 16]. This approach has been recently identified [17] as more appropriate in a short-term range due to the difficulty of the industry to embrace complex and emerging control methods like reinforcement learning [18, 19].

The proposed algorithm extends the basic formulation of [16] to encompass the control algorithm around a single indicator. The indicator puts in relation a possible action (like increasing the electricity fed to a HP), the corresponding gain in operating expense, and the heat production gain. Our heuristic control algorithm (HCA) evaluates this indicator as often as needed and chooses the action which minimizes this indicator. Such an approach is novel because it doesn't require any parameters tuning and achieve the close-to-optimal control trajectory.

1.3 Description

This work is organized as follows: Section 3 provides a description of the system model and the HCA. The methodology for the benchmark of the algorithm is also provided. Section 4 describes the case study and the main cost and model parameters. The benchmark results are exposed in section 5, while the conclusions of this work are presented in section 6.

2 Achievement of Deliverable

2.1 Date

This deliverable is handed in December 2020.

2.2 Demonstration of the Deliverable

The deliverable aims to apply to any buildings with HP and PV in Switzerland and outside. The dataset of building used in this work is based on the cantonal buildings registry of the canton of Vaud from which all buildings of the Rolle demonstrator and surrounding are extracted. The considered buildings, although anonymized, are real buildings from which their properties are extracted using the Swiss society of engineer and architects (SIA) norm.

2.4 Impact

Starting from the building model formulation and the control problem, this work can very rapidly turn into a real product and be implemented into HP control hardware. The current Swiss market suffers from a lack of such products.

3 Methodology

This section presents the methodology to benchmark the HCA against the solution solved by a MILP formulation. The same building energy system model, described in section 3.1, is used in both approaches. Then section 3.2 detailed the objective function of the MILP formulation, followed by the workflow of the HCA introduced in section 3.3. Finally, section 3.4, gives the benchmark methodology and the key performance indicator definitions.

3.1 System model

The considered energy system, illustrated in Figure 2, comprises an air-water HP, with variable operating power capability, dedicated to DHW and building heating coupled with a PV installation. The HP is augmented with an electric heater (EH) to cover any peak demand in any extreme case. The building is connected to electrical networks and can import and export electricity if required. The local electricity consumption should be satisfied at any time. The heating demand should be met so that the building and hot water tank temperature stay within given bounds.

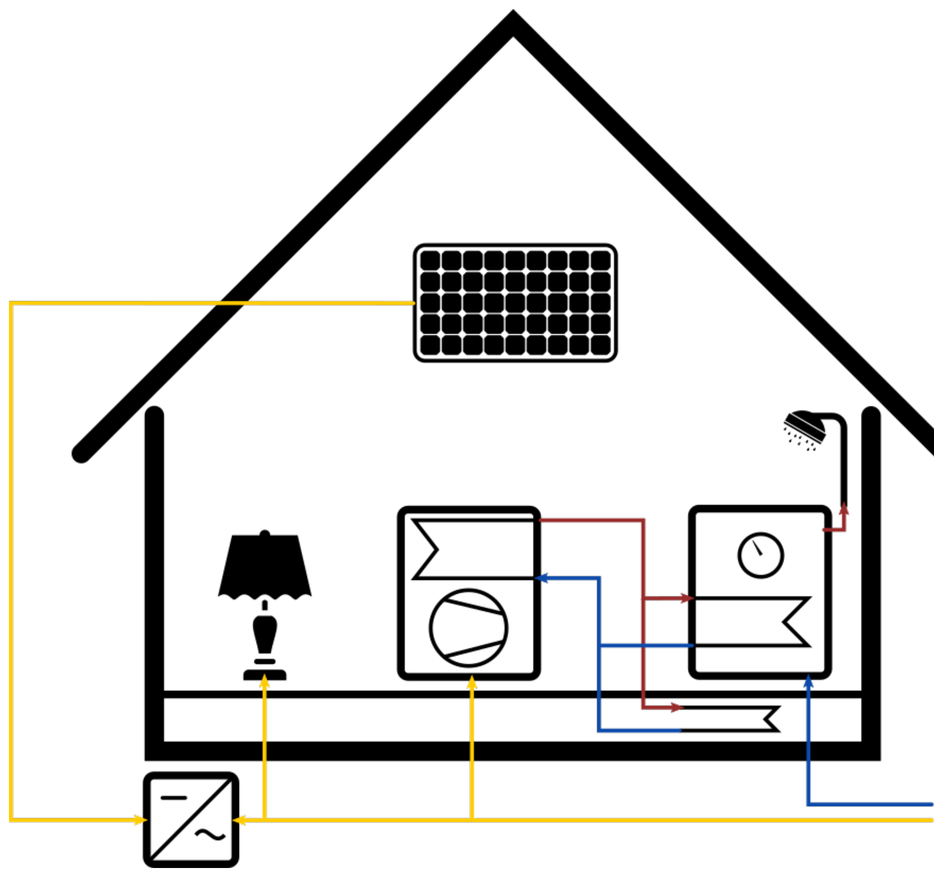

Figure 2: A basic sketch of the system under study

This section presents a linear model of this energy system that can be solved either with a MILP formulation or with the HCA. A linear model is used to ensure a fair performance benchmark, although the HCA would work with any non-linear model. This model is derived from a previous work in which the optimal sizing of the PV and battery capacity was performed [20]. In this work, we introduce a thermal model and perform the optimization of the HP and EH size. Although a battery could be considered in the formulation of the problem, it is omitted in this work for simplicity. The active power curtailment is modeled as a controllable load with an upper bound equal to the instantaneous PV generation. The complete set of variables are provided in Table 1. In the latter, the decision variables (in opposition to parameters) are marked with a $\star$.

Table 1: Variables definition. The decision variables are indicated with a $\star$ in the **V** columns. The rest are parameters.

	Variables	Set	Units	V	Descriptions
TIME	T	$\mathbb{N}$	-		number of time steps
	TS	$\mathbb{R}_+^T$	s		time steps
SYSTEM	P^{imp}	$\mathbb{R}_+^T$	W	$\star$	imported power (from the grid)
	P^{exp}	$\mathbb{R}_+^T$	W	$\star$	exported power (to the grid)
	P^{load}	$\mathbb{R}_+^T$	W		uncontrollable electricity consumption
	P^{cur}	$\mathbb{R}_+^T$	W	$\star$	curtailed power
	T^{amb}	$\mathbb{R}_+^T$	K		ambient/external temperature
	c^{imp}	$\mathbb{R}_+^T$	CHF/J		import electricity tariff
	c^{exp}	$\mathbb{R}_+^T$	CHF/J		export electricity tariff
	L	$\mathbb{N}$	years		system lifetime
	r	$\mathbb{R}$	-		discount rate
PV	N	$\mathbb{N}$	-		number of PV configurations
	J	$\mathbb{N}$	-		number of roofs
	n^{mod}	$\mathbb{N}^N$	-	$\star$	PV configurations, number of units
	b^{mod}	$\{0,1\}^N$	-	$\star$	PV configurations, presences
	b^{pv}	$\{0,1\}$	-	$\star$	PV installation, presence
	c_F^{PV}	$\mathbb{R}_+$	CHF		PV fixed cost
	c^{mod}	$\mathbb{R}_+^N$	CHF/W		PV configurations, specific costs
	$P_{\text{nom}}^{\text{mod}}$	$\mathbb{R}_+^N$	W		PV unit nominal powers
	P_t^{PV}	$\mathbb{R}_+^{T\times N}$	W		PV configuration unit generations
	A^{mod}	$\mathbb{R}_+^N$	m^2		PV configuration areas
	A^{roof}	$\mathbb{R}_+^J$	m^2		roofs areas
HP	$P_{\text{cap}}^{\text{hp}}$	$\mathbb{R}_+$	W	$\star$	HP electric nominal power
	$P_{\text{cap}}^{\text{el}}$	$\mathbb{R}_+$	W	$\star$	EH nominal power
	P^{hp}	$\mathbb{R}_+^T$	W	$\star$	HP electric power
	P^{el}	$\mathbb{R}_+^T$	W	$\star$	EH power
	$\dot{Q}^{\text{hp}}$	$\mathbb{R}_+^T$	W	$\star$	HP thermal power
	COP	$\mathbb{R}_+^T$	W		HP coefficient of performance
	q^{carnot}	$\mathbb{R}_+$	-		carnot non-ideality factor of the HP
	S_t	$\mathbb{R}_+^T$			HP starting up
	R_t	$\mathbb{R}_+^T$			HP running
	c^{start}	$\mathbb{R}_+$	CHF		HP start cost
	c^{run}	$\mathbb{R}_+$	CHF/s		HP run cost
	c^{hp}	$\mathbb{R}_+$	CHF/W		HP specific cost
	c^{el}	$\mathbb{R}_+$	CHF/W		EH specific cost
	η^{el}	$\mathbb{R}_+$	-		EH efficiency
DHW	$\dot{Q}^{\text{hp}\to\text{tank}}$	$\mathbb{R}_+^T$	W	$\star$	HP thermal power to tank
	$\dot{Q}^{\text{el}\to\text{tank}}$	$\mathbb{R}_+^T$	W	$\star$	EH thermal power to tank
	$\dot{Q}^{\text{DHW}}$	$\mathbb{R}_+^T$	W		DHW thermal power consumption
	T^{tank}	$\mathbb{R}_+^T$	K	$\star$	tank temperature
	T^{room}	$\mathbb{R}_+$	K		room temperature (constant)
	$T^{\text{H,tank}}$	$\mathbb{R}_+$	K		hot source temperature of the domestic hot water circuit
	$T_{\text{min,max}}^{\text{tank}}$	$\mathbb{R}_+$	K		hot water tank service temperature range
	C^{tank}	$\mathbb{R}_+$	J/K		thermal equivalent capacitance of the dhw tank
	R^{tank}	$\mathbb{R}_+$	K/W		thermal equivalent resistance of the DHW tank
BUILDING	$\dot{Q}^{\text{hp}\to\text{sh}}$	$\mathbb{R}_+^T$	W	$\star$	HP thermal power to space heating
	$\dot{Q}^{\text{el}\to\text{sh}}$	$\mathbb{R}_+^T$	W	$\star$	EH thermal power to space heating
	$\dot{Q}^{\text{sh}\to\text{b}}$	$\mathbb{R}_+^T$	W		thermal power from the space heating to building
	T^{b}	$\mathbb{R}_+^T$	K	$\star$	building temperature
	T^{sh}	$\mathbb{R}_+^T$	K	$\star$	space heating temperature
	$T^{\text{H,sh}}$	$\mathbb{R}_+$	K		hot source temperature of the space heating circuit
	$T_{\text{min,max}}^{\text{b}}$	$\mathbb{R}_+^T$	K		building comfort temperature range
	$T_{\text{min,max}}^{\text{sh}}$	$\mathbb{R}_+^T$	K		space heating service temperature range
	C^{sh}	$\mathbb{R}_+$	J/K		thermal equivalent capacitance of the space heating
	C^{b}	$\mathbb{R}_+$	J/K		thermal equivalent capacitance of the building
	R^{sh}	$\mathbb{R}_+$	K/W		thermal equivalent resistance of the space heating
	R^{b}	$\mathbb{R}_+$	K/W		thermal equivalent resistance of the building
	A_0	$\mathbb{R}_+$	m^2		equivalent horizontal building opening surface

The system's power balance is described in (1) and must be satisfied for all time steps. The PV system's modeling equations are described in eqs. (2a) to (2c).

$$P_t^{\mathrm{imp}} - P_t^{\mathrm{exp}} + P_t^{\mathrm{cur}} + P_t^{\mathrm{PV}} - P_t^{\mathrm{hp}} - P_t^{\mathrm{el}} = P_t^{\mathrm{load}} \quad \forall t \in T \tag{1}$$

PV generation at time t	$P_t^{\mathrm{PV}} = \sum_{i=1}^{N} P_{t,i}^{\mathrm{mod}} \cdot n_i^{\mathrm{mod}}$	(2a)
area constraints for all roofs $\in J$	$\sum_{i=1}^{N_j} n_i^{\mathrm{mod}} \cdot A_i^{\mathrm{mod}} < A_j^{\mathrm{roof}} \quad \forall j \in J$	(2b)
curtailment constraint	$P_t^{\mathrm{cur}} - P_t^{\mathrm{PV}} < 0$	(2c)

The thermal model is based on the electrical-thermal analogy. The reference circuit is pictured in Figure 3. The circuit consists of the HP (and EH, omitted for clarity) providing heat to a space heating circuit which as its thermal inertia (equivalent capacitance) and transfers its heat (3c) to the building. The latter gains heat from the solar irradiance (through windows) (3e) and loses heat in the surrounding environment (3d). This is represented in the heat balance equation of the building (3a). The building temperature is constrained by applying reasonable bounds (3f) to ensure a fair approximation of the occupants' comfort while guaranteeing the optimization feasibility. The initial temperature must also be specified (3h).

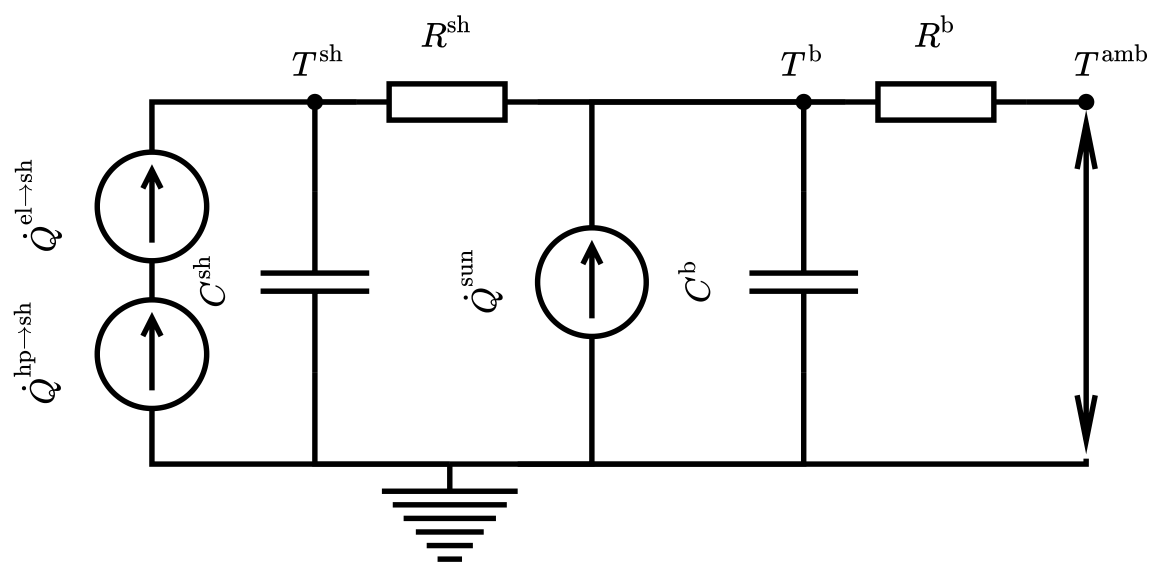

Figure 3: Equivalent electrical circuit of the building and space heating circuit

building thermal balance	$C^{\mathrm{b}} \cdot \dfrac{T_t^{\mathrm{b}} - T_{t-1}^{\mathrm{b}}}{\mathrm{TS}_t} = \dot{Q}_t^{\mathrm{sh}\to\mathrm{b}} - \dot{Q}_t^{\mathrm{loss,b}} + \dot{Q}_t^{\mathrm{sun}}$	(3a)
space heating thermal balance	$C^{\mathrm{sh}} \cdot \dfrac{T_t^{\mathrm{sh}} - T_{t-1}^{\mathrm{sh}}}{\mathrm{TS}_t} = -\dot{Q}_t^{\mathrm{sh}\to\mathrm{b}} + \dot{Q}_t^{\mathrm{el}\to\mathrm{sh}} + \dot{Q}_t^{\mathrm{hp}\to\mathrm{sh}}$	(3b)
heat gain from the space heating circuit	$\dot{Q}_t^{\mathrm{sh}\to\mathrm{b}} = \dfrac{T_t^{\mathrm{sh}} - T_t^{\mathrm{b}}}{R^{\mathrm{sh}}}$	(3c)
heat loss in the surrounding environment	$\dot{Q}_t^{\mathrm{loss,b}} = \dfrac{T_t^{\mathrm{b}} - T_t^{\mathrm{amb}}}{R^{\mathrm{b}}}$	(3d)
heat gain from the sun	$\dot{Q}_t^{\mathrm{sun}} = I_{0,t} A_0^{\mathrm{sun}}$	(3e)
building temperature constraints	$T_{\mathrm{min}}^{\mathrm{b}} \leq T_t^{\mathrm{b}} \leq \max(T_{\mathrm{max}}^{\mathrm{b}}, T_t^{\mathrm{amb}})$	(3f)
space heating temperature constraint	$T_{\mathrm{min}}^{\mathrm{sh}} \leq T_t^{\mathrm{sh}} \leq T_{\mathrm{max}}^{\mathrm{sh}}$	(3g)
initial building temperature constraint	$T_0^{\mathrm{b}} = T_{\mathrm{init}}^{\mathrm{b}}$	(3h)
initial space hating temperature constraint	$T_0^{\mathrm{sh}} = T_{\mathrm{init}}^{\mathrm{sh}}$	(3i)

To fulfill the domestic hot water demand ($\dot{Q}_t^{\mathrm{DHW}}$), the hot water tank acts as a thermal reservoir, which is supplied by the HP and EH (see thermal balance equation (4a)). The tank heat loss depends only on the tank temperature (4b), the surrounding temperature, T_t^{room} is assumed as constant à 20 °C. The temperature in the tank is bounded (4c). The tank heat loss is not considered as heat gain for the building. Hence, the tank is a non-ideal storage (3).

tank heat balance	$C^{\mathrm{tank}} \cdot \dfrac{\left(T_t^{\mathrm{tank}} - T_{t-1}^{\mathrm{tank}}\right)}{\mathrm{TS}_t} = \dot{Q}_t^{\mathrm{el}\to\mathrm{tank}} + \dot{Q}_t^{\mathrm{hp}\to\mathrm{tank}} - \dot{Q}_t^{\mathrm{loss,t}} - \dot{Q}_t^{\mathrm{DHW}}$	(4a)
heat loss from the tank	$\dot{Q}_t^{\mathrm{loss,t}} = \dfrac{T_t^{\mathrm{tank}} - T_t^{\mathrm{room}}}{R^{\mathrm{tank}}}$	(4b)
tank temp. constraint	$T_{\mathrm{min}}^{\mathrm{tank}} \leq T_t^{\mathrm{tank}} \leq T_{\mathrm{max}}^{\mathrm{tank}}$	(4c)

To provide the required heat in both the space heating circuit and the DHW tank circuit, the HP and EH consume electric power as described in (5a) and (5b). The coefficient of performance (COP) is derived from the Carnot definition and assume constant hot and cold source temperature (both for the space heating and tank side) (5c) and (5d). The maximum input power demand defines the unit's capacity for both the HP and the EH (5e) and (5f).

electric power for the HP	$$P_t^{\text{hp}} = \frac{\dot{Q}_t^{\text{hp}\to\text{sh}}}{COP_t^{\text{sh}}} + \frac{\dot{Q}_t^{\text{hp}\to\text{tank}}}{COP_t^{\text{dhw}}}$$	(5a)
electric power for the EH	$$P_t^{\text{el}} = \frac{\dot{Q}^{\text{el}\to\text{sh}} + \dot{Q}_t^{\text{el}\to\text{tank}}}{\eta^{\text{el}}}$$	(5b)
COP for space heating	$$COP_t^{\text{sh}} = q^{\text{carnot}} \cdot \frac{T^{\text{H,sh}}}{T^{\text{H,sh}} - T_t^{\text{amb}}}$$	(5c)
COP for the DHW tank	$$COP_t^{\text{dhw}} = q^{\text{carnot}} \cdot \frac{T^{\text{H,tank}}}{T^{\text{H,tank}} - T_t^{\text{amb}}}$$	(5d)
HP capacity constraint	$$P_{\text{cap}}^{\text{hp}} \geq \frac{\dot{Q}_t^{\text{hp}\to\text{sh}}}{COP_t^{\text{sh}}} + \frac{\dot{Q}_t^{\text{hp}\to\text{tank}}}{COP_t^{\text{dhw}}}$$	(5e)
EH capacity constraint	$$P_{\text{cap}}^{\text{el}} \geq \frac{\dot{Q}^{\text{el}\to\text{sh}} + \dot{Q}_t^{\text{el}\to\text{tank}}}{\eta^{\text{el}}}$$	(5f)

3.2 MILP formulation

The problem is formulated as a mixed-integer linear problem, in which the objective function is to minimize the total cost of ownership (7).

$$\text{minimize} \quad TOTEX \quad \text{subject to eqs. (1) to (5f)} \tag{6}$$

The $TOTEX$ is composed of the capital (9), which include the cost of buying PV modules, a HP and the battery (11), and operating cost (8), which consist of the maintenance cost of the PV installation, the operating cost of the HP and electrical boiler, and the cost of exchanging energy with the grid (12). In this work, only a standard volumetric tariff is defined.

$$TOTEX = OPEX + R \cdot CAPEX \tag{7}$$

$$OPEX = \text{ox}_{\text{ge}} + \text{ox}_{\text{hpo}} + \text{ox}_{\text{elo}} + \text{ox}_{\text{pm}} \tag{8}$$

$$CAPEX = \text{cx}_{\text{pv}} + \text{cx}_{\text{hp}} + \text{cx}_{\text{el}} \tag{9}$$

$$R = \frac{r \cdot (1+r)^L}{(1+r)^L - 1} \tag{10}$$

The $CAPEX$ components are defined in (11).

PV	$$\text{cx}_{\text{pv}} = \sum_{i=1}^{N} n_i^{\text{mod}} \cdot P_{\text{nom},i}^{\text{mod}} \cdot c_i^{\text{mod}} + b^{\text{pv}} \cdot c_F^{\text{PV}}$$	(11a)
HP	$$\text{cx}_{\text{hp}} = P_{\text{cap}}^{\text{hp}} \cdot c^{\text{hp}}$$	(11b)
EH	$$\text{cx}_{\text{el}} = P_{\text{cap}}^{\text{el}} \cdot c^{\text{el}}$$	(11c)

The *OPEX* components are defined in (12).

grid exchanges	$\mathrm{ox}_{\mathrm{ge}} = \sum_{t=1}^{T} \left[P_t^{\mathrm{imp}} \cdot c_t^{\mathrm{exp}} - P_t^{\mathrm{exp}} \cdot c_t^{\mathrm{imp}} \right] \cdot \mathrm{TS}_t$	(12a)
pv maintenance	$\mathrm{ox}_{\mathrm{pm}} = \gamma^{\mathrm{PV}} \cdot \mathrm{cx}_{\mathrm{pv}}$	(12b)

3.3 HCA formulation

The HCA's objective is to optimize the HP power consumption P_t^{hp} to meet the DHW and building heating needs while minimizing the *OPEX*. This power consumption profile is discretized with a power step ΔP^{hp}. The algorithm's main phases, shown in Figure 4, are first to initialize temperatures, then optimize the HP operation to meet the DHW needs, and finally, a second optimization is performed to meet the building heating demand.

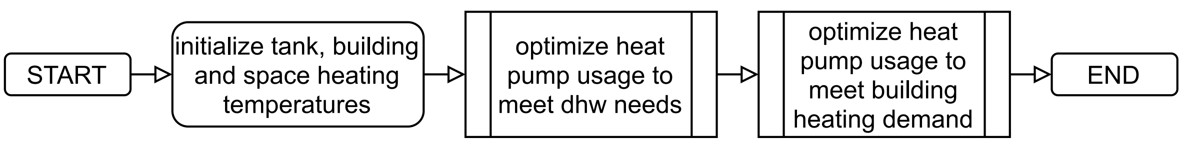

Figure 4: Main steps of the HCA

The HCA, detailed in Figure 5, is used to optimize the HP usage to meet either the DHW or building heating demand. For the following, the word *tank* can be exchanged by *building*. At the beginning of the process, both HP and EH power profiles are set to zero. A first heat balance of the tank is carried out (thanks to eqs. (3a) to (5f)), enabling to obtain the temperature profile of the tank over the entire time horizon. An indicator is then computed (13) for every possible increase of the HP electric power. If the tank temperature drops below the minimum temperature, a period P is defined, corresponding to the period during which the HP power should be increased to maintain the tank temperature in a given range $[T_{\mathrm{min}}^{\mathrm{tank}}, T_{\mathrm{max}}^{\mathrm{tank}}]$. If the HP is not already used at nominal power during the period P, then the HP power $P_{t_{\mathrm{heat}}}^{\mathrm{hp}}$ is increased by a power step ΔP^{hp} at the time t_{heat} corresponding to the minimum of the indicator. If the HP was already at maximum power during the period P, then the EH is used instead. A new heat balance is carried out to assess the tank's temperature rise from t_{heat} to the end of the time horizon. If the tank temperature is still too low, the loop starts again.

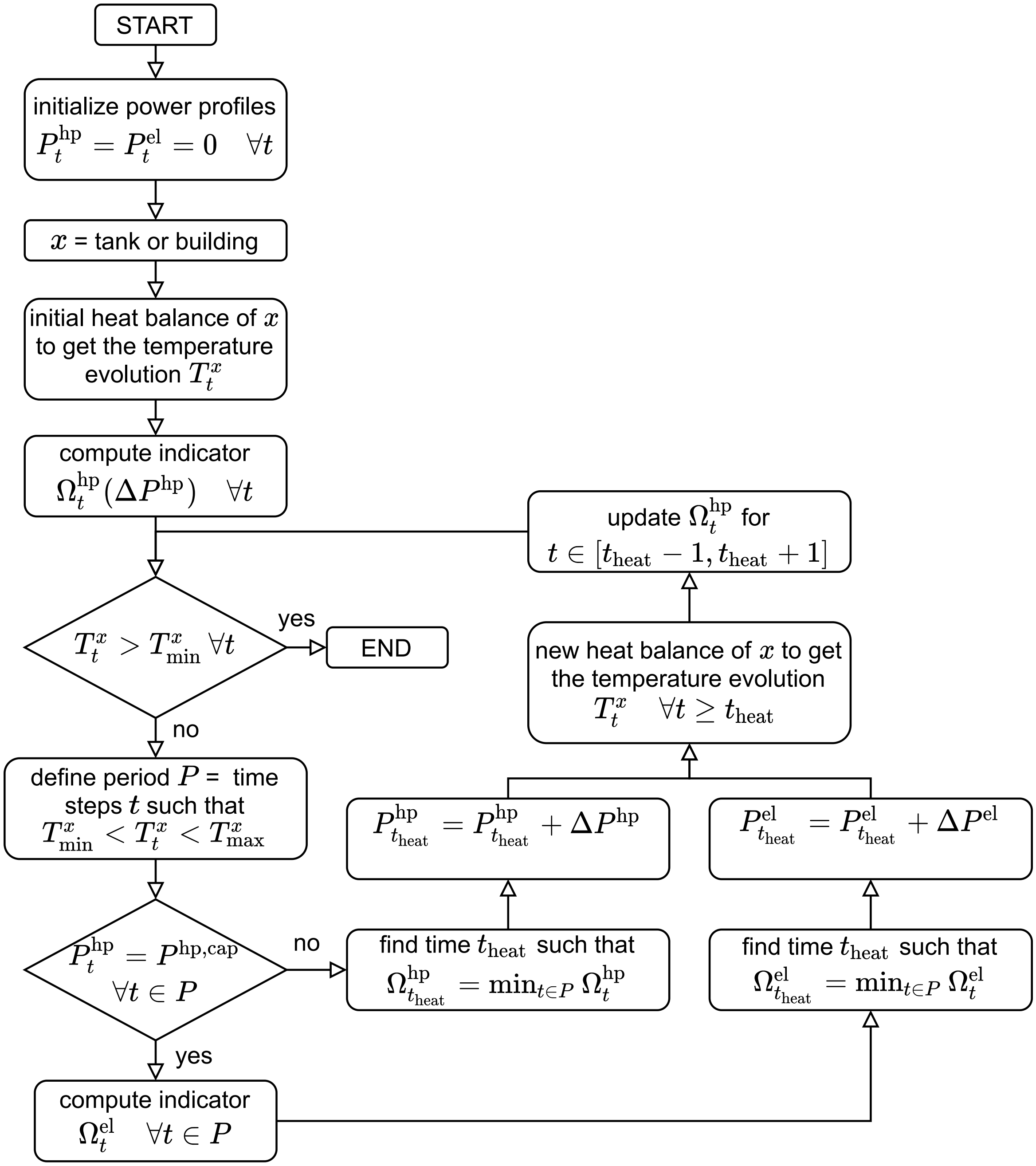

Figure 5: Optimal HP and EH control

The HP indicator Ω_t^{hp} gives the cost of the produced heat. In other words, it is the ratio between the $OPEX$ increase and thermal energy production increase due to the rise of the HP electricity consumption by ΔP^{hp}.

$$\Omega_t^{\text{hp}} = \frac{\Delta OPEX_t}{\Delta Q_t} \tag{13}$$

Here, the $OPEX$ is the sum of two contributions. The first part, given by the power exchange with the grid, takes into account the import c_t^{imp} and export c_t^{exp} electricity tariffs.

$$OPEX_t = OPEX_t^{\text{grid}} + OPEX_t^{\text{hp}} \tag{14a}$$

$$OPEX_t^{\text{grid}} = \left(P_t^{\text{imp}} \cdot c_t^{\text{imp}} - P_t^{\text{exp}} \cdot c_t^{\text{exp}}\right) \cdot \text{TS}_t \tag{14b}$$

$$OPEX_t^{\text{hp}} = c^{\text{start}} \cdot S_t + c^{\text{run}} \cdot R_t \cdot \text{TS}_t \tag{14c}$$

The second part, $OPEX_t^{\text{hp}}$, depends on the HP operation. It consists of two parts, a cost for each start-up of the HP and a second, proportional to the HP operation duration. The running state R_t and starting S_t are defined as followed.

$$R_t = \begin{cases} 1 & \text{if } P_t^{\text{hp}} > 0 \\ 0 & \text{otherwise} \end{cases} \tag{15}$$

$$S_t = \begin{cases} 1 & \text{if } R_{t-1} = 0 \cap R_t = 1 \\ 0 & \text{otherwise} \end{cases} \tag{16}$$

Finally, the $\Delta OPEX_t$ is given by the $OPEX$ difference when considering an increase of the HP power consumption by a power step ΔP^{hp}. This increase of the power consumption as an influence on the $OPEX_t^{\text{grid}}$ through (1) and obviously on $OPEX_t^{\text{hp}}$ since R_t and S_t depends directly on P_t^{hp}.

$$\Delta OPEX_t = OPEX_t(P_t^{\text{hp}} + \Delta P^{\text{hp}}) - OPEX_t(P_t^{\text{hp}}) \tag{17}$$

The denominator of the indicator is based on the heat generated by the HP, $\dot{Q}_t^{\text{hp}}$, defined as :

$$\dot{Q}_t^{\text{hp}}(P_t^{\text{hp}}) = P_t^{\text{hp}} \cdot COP_t(P_t^{\text{hp}}) \cdot \text{TS}_t \tag{18}$$

Thus a variation of the heat generation driven by an increase of the HP consumption ΔP^{hp} can be expressed as :

$$\Delta\dot{Q}_t^{\text{hp}} = \dot{Q}_t^{\text{hp}}(P_t^{\text{hp}} + \Delta P^{\text{hp}}) - \dot{Q}_t^{\text{hp}}(P_t^{\text{hp}}) \tag{19}$$

$$= \Big((P_t^{\text{hp}} + \Delta P^{\text{hp}})) \cdot COP_t(P_t^{\text{hp}} + \Delta P^{\text{hp}}) - P_t^{\text{hp}} \cdot COP_t(P_t^{\text{hp}})\Big) \cdot \text{TS}_t \tag{20}$$

For this benchmark, the COP formulation is defined in eqs. (5c) and (5d) was implemented in the HCA too. In this way, the COP is a parameter that doesn't depend on any decision variable. However, this is a simplistic assumption. Usually, the COP depends on the hot source temperature and part load ratio of the HP. The following gives an example of such a non-linear formulation that can be easily implemented in the HCA.

$$COP_{\text{nonlin}}\left(T_t^{\text{amb}}, T_t^H, P_t^{\text{hp,n}}\right) = COP_{\text{lin}}\left(T_t^{\text{amb}}, T_t^H\right) \cdot f_c\left(P_t^{\text{hp,n}}\right) \tag{21}$$

With T^H, the tank T^{tank} or building T^{b} temperature. The linear part of the COP is only a linear function of the external temperature T^{amb} and hot source temperature T^H.

$$COP_{\text{lin}}\left(T_t^{\text{amb}}, T_t^H\right) = d_0 + d_1 \cdot T_t^{\text{amb}} + d_2 \cdot T_t^H \tag{22}$$

And f_c is the dependence of the HP efficiency on its part load ratio, here expressed with six order polynomial function.

$$f_c\left(P_t^{\text{hp}}\right) = \sum_{n=1}^{6} a_n \cdot \left(P_t^{\text{hp,n}}\right)^n \tag{23}$$

Where $P_t^{\text{hp,n}}$ is the normalized HP power.

$$P_t^{\text{hp,n}} = \frac{P_t^{\text{hp}}}{P_{\text{cap}}^{\text{hp}}} \tag{24}$$

3.4 Benchmark

In order to benchmark the HCA performance, the algorithm is applied to various representative buildings. The methodology for selecting the set of representative buildings is described below. For each building in this set, typical periods are defined based on the irradiance, temperature, electrical, and DHW consumption. Then for each of these periods (and each building), the HP operation is solved using both the HCA and MILP formulation. Finally, key performance metrics are computed based on the operation results. This process is graphically summarized in Figure 6. The following will describe in more detail each of these steps.

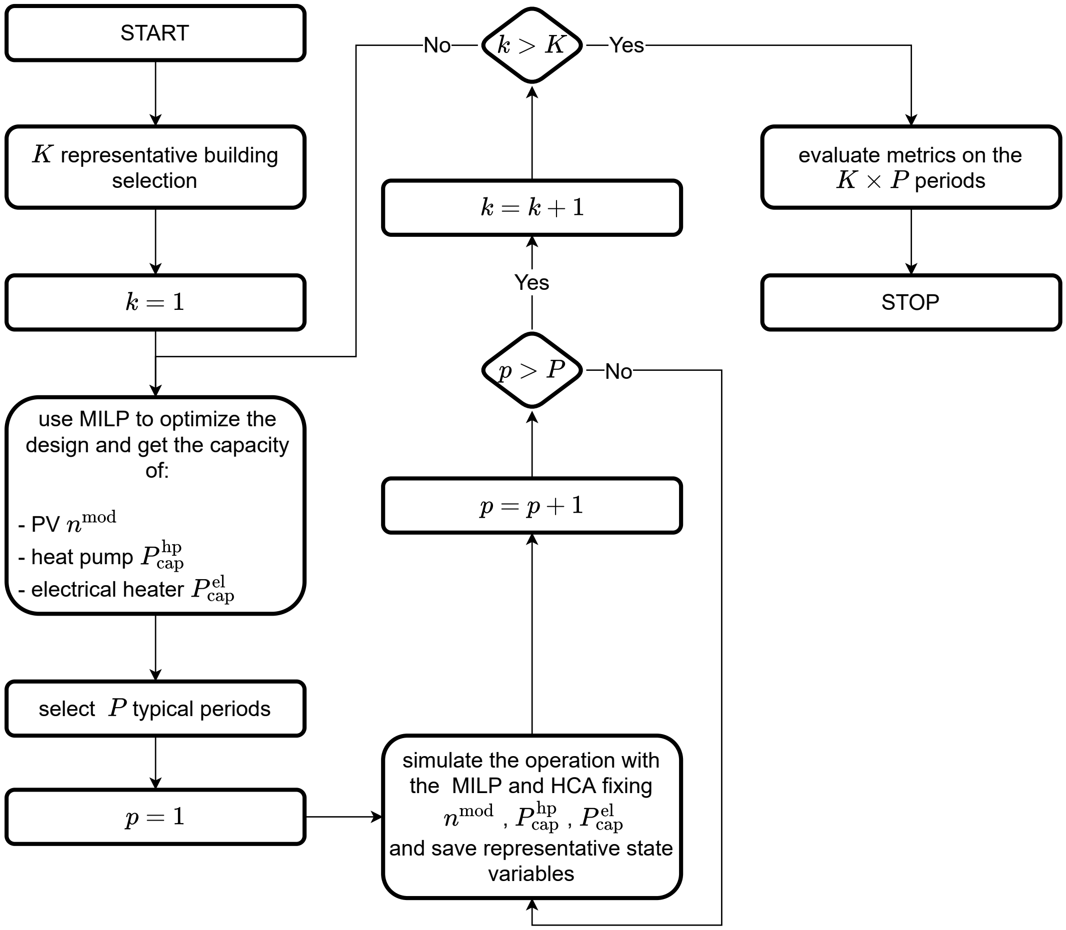

Figure 6: Workflow of the benchmark process

The cantonal buildings registry (RCB) or its federal version (RegBL)[1] gives standard information about all the buildings in the canton, like footprint area, number of levels, building or renovation year, number of housing, etc. The RCB divides the buildings into six categories:

1010 provisional building

1021 single-family house

1025 multi-family building

1030 multi-family building with annex activities (like shops)

1040 building with partial usage for housing

1060 non-residential building.

[1] https://www.housing-stat.ch/fr/accueil.html

By combining the building category, footprint area, the number of levels, number of housing, and the renovation year with the SIA norm 2024 [21], it is possible to extract:

1. an estimation of the electrical, heat, and domestic hot water demand
2. the physical properties of the building (heat transfer coefficient, thermal capacity, etc.(see Table 1).

From the *solar roof* [2] data, the roofs' characteristics (area, azimuth, and tilt) are also known for each building. From this dataset of buildings, the most representative buildings are extracted for each building category. The *k-medoids* [22] algorithm is used to perform the clustering on the following set of building features:

- number of housing
- number of levels
- building renovation year
- building height
- building footprint area
- the ratio between the annual PV potential (extracted from *solar roof*) and the annual electricity demand
- the total heat demand (including DHW)

The number of medoids (representative building) is a parameter of the clustering. Finally, for all medoids, electrical and DHW load profiles are allocated using the annual energy demands. The electric profiles come from an database of load profiles acquired during a project on the households' flexibility [23, 24]. The DHW load consumptions are generated from daily samples extracted from the work of Roux and Booysen [25, 26]. For these representative buildings, the PV, HP, and EH capacities will be optimized at the same time as their operations for one full year by solving the MILP problem depicted in section 3.2. To investigate the HCA's operational behavior, typical periods have to be defined.

Following a similar approach, the typical periods' selection for a particular building consists in choosing a few representative period samples from a set of time-series samples. This approach and the complexity of energy systems is discussed in detail in [27]. The partitioning of long time-series into representative shorter samples is now a well-accepted technique [28, 29]. The first step is, hence, to cut the time series into samples. In this work, each time-series sample is one week long. There are thus, 52 time-series samples for a particular building. Each sample consists of a $T^S \times F$ matrix, where T^S is the length of the time series (corresponding to one week in this case), and F is the number of considered features. For

[2] https://www.uvek-gis.admin.ch/BFE/sonnendach

the latter, we choose the electrical load P^{load}, the DHW demand $\dot{Q}^{\mathrm{DHW}}$, the horizontal global irradiance GHI, and the ambient temperature T^{amb}. Again, the *k-medoids*[22] algorithm was used to extract four representative weeks from the 52 available.

Once the design of a particular building in terms of technology capacity and the corresponding typical weeks are defined, the system operation is simulated. First, a reference operation is obtained by solving the MILP of 3.2. Then the HCA is run. The relevant performance metrics can be computed for each typical week and for each representative building.

The performance metrics are defined for each building $k \in [1...K]$ and each typical period $p \in [1...P]$. For easing the notation, the subscript k, p are dropped. The operator $\sum$ denotes the operation $\sum_{t=1}^{T^S}$.

operating cost	$OPEX = \sum (P_t^{\mathrm{imp}} \cdot c_t^{\mathrm{imp}} - P_t^{\mathrm{exp}} \cdot c_t^{\mathrm{exp}}) \mathrm{TS}_t$	(25a)
heat generation	$Q_{u,s} = \sum Q_t^{u,s} \cdot \mathrm{TS}_t \quad \forall\, u \in [\mathrm{hp}, \mathrm{el}],\ s \in [\mathrm{sh}, \mathrm{tank}]$	(25b)
HP running time ratio	$\mathrm{HP}_{\mathrm{run}} = \dfrac{\sum R_t \cdot \mathrm{TS}_t}{\sum \mathrm{TS}_t}$ with R_t defined in 15	(25c)
HP switch on per day	$\mathrm{HP}_{\mathrm{switch}} = \dfrac{\sum S_t}{\sum \mathrm{TS}_t / (24 \cdot 3600)}$ with S_t defined in 16	(25d)
temperature deviation	$\Delta \bar{T} = \dfrac{\sum \lvert T_t^{\mathrm{b}} - T^* \rvert}{T^S}$ with $T^* = 19\,^{\circ}\mathrm{C}$	(25e)

The time needed for both algorithms to simulate the operation for a typical week is also recorded.

4 Case study

The cantonal building registry of the canton of Vaud has been used as the building data set. Five representative buildings are extracted for each of the following categories

- Single-family house (cat 1021)
- Multi-family building (cat 1025)
- Non-residential building (cat 1060)

The resulting 15 representative buildings are pictured in Figure 7. This figure shows the total exergy demand (defined in equation 26) versus the building footage: the building footprint times the number of levels. The size of the disc represents the PV potential capacity.

$$B_k = \sum_{t=1}^{T} \left[P_{k,t}^{\mathrm{load}} + \dot{Q}_{k,t}^{\mathrm{DHW}} \left(1 - \frac{T^*}{T^{\mathrm{dhw}}}\right) + Q_{k,t}^{\mathrm{sh}} \left(1 - \frac{T^*}{T_k^{\mathrm{sh}}}\right) \right] \mathrm{TS}_t \quad \forall k = 1...K \tag{26}$$

where $T^* = 19 + 273\,K$, $T^{\text{dhw}} = 60 + 273\,K$ and T_k^{sh} depends on the year of construction of the building, and vary between 35 and 50 °C.

As highlighted in Figure 7, single-family houses are relatively small compared to multi-family and non-residential buildings. Non-residential buildings can have small building footprint but a high exergy demand, while multi-family buildings have the exergy demand scaling linearly with the building footprint. As a matter of fact, the reason behind this is that non-residential buildings have an energy consumption that is uncorrelated with their building footprint (industry sites or shopping malls), while residential buildings energy demand scale typically with the living surface (the more surface, the more people, the more energy needs). The use of the exergy demand in this figure is simply to aggregate the electric consumption, the heat need for space heating, and the DHW consumption in one single metric.

The buildings' PV related data are summarized in Table 3. The buildings' thermal parameters are summarized in Table 4. The cost for PV and HP are estimated using the approach reported in [20], while the HP and EH cost comes from [30] and [31]. The cost parameters and other standard parameters are reported in Table 2.

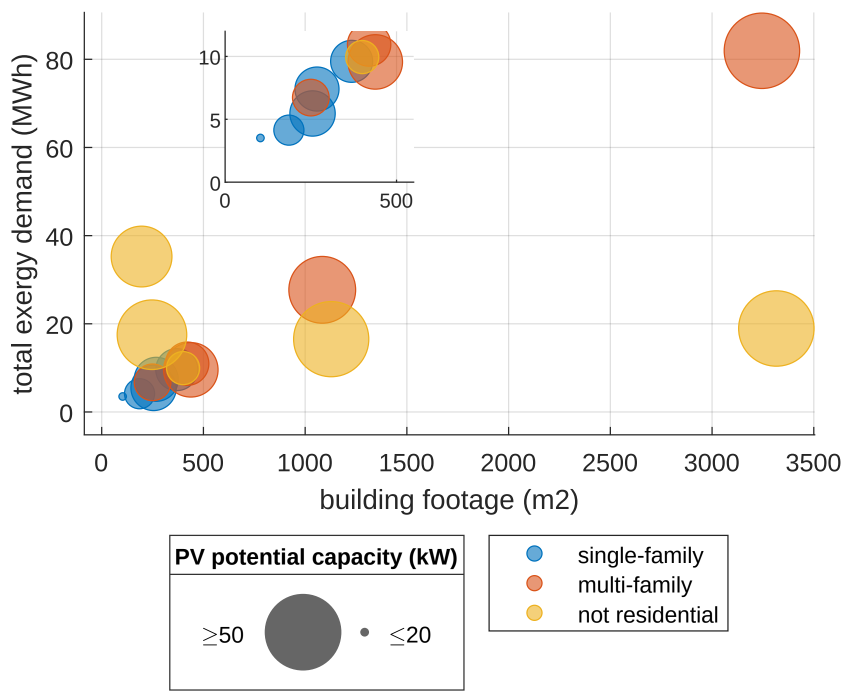

Figure 7: Systems size given by their exergy consumption and buildings footage. The size of the disc indicates the PV potential capacity.

Table 2: PV, HP, and system parameters

	Parameter	Unit	Value
PV	c_F^{PV}	CHF	10'050
	c^{mod}	CHF/W	0.83
	$P_{\mathrm{nom}}^{\mathrm{mod}}$	W	315
	P_t^{PV}	W	[1]
	A^{mod}	m^2	1.6
	γ^{PV}	-	0.5%
Thermal	$\bar{U}^{\mathrm{tank}}$	$\mathrm{W/m^2K}$	1.0
	q^{carnot}	-	0.8
	η^{el}	-	0.99
	c^{hp}	CHF/W	1.5
	T^{amb}	K	[2]
	$T^{\mathrm{H,tank}}$	°C	90
	$T_{\mathrm{min,max}}^{\mathrm{b}}$	°C	> 19
	$T_{\mathrm{min}}^{\mathrm{sh}}$	°C	5
	$T_{\mathrm{min,max}}^{\mathrm{tank}}$	°C	59-85
System	T	-	[3]
	TS	s	900
	L	years	25
	r	-	3%
	P^{load}	W	[4]
	$\dot{Q}_t^{\mathrm{DHW}}$	W	[4]

[1] Simulated using pvlib for each configuration according to the modules parameters
[2] Extracted from weather data from *meteo-suisse*[3].
[3] 35040 for the design phase and 672 per periods for the simulations
[4] Allocated for each building from a source of real measurement

Table 3: Building PV parameters

		$P^{\mathrm{PV}}_{\mathrm{cap,pot}}$ kW	A^{roof} m^2	N -	J -
House	1	28	211	5	5
	2	29	215	4	4
	3	19	141	2	2
	4	23	180	6	6
	5	29	225	6	6
Multi family	6	26	195	6	6
	7	34	262	8	8
	8	43	314	4	1
	9	28	216	6	6
	10	96	716	3	3
Commercial	11	50	381	23	14
	12	110	803	4	1
	13	38	287	2	2
	14	45	337	2	2
	15	24	181	2	2

Table 4: Building thermal parameters

		C^{b} $\frac{\mathrm{kWh}}{\mathrm{K}}$	C^{sh} $\frac{\mathrm{kWh}}{\mathrm{K}}$	$U^{\mathrm{b}*}$ $\frac{\mathrm{W}}{\mathrm{K}}$	$U^{\mathrm{sh}*}$ $\frac{\mathrm{W}}{\mathrm{K}}$	$U^{\mathrm{tank}*}$ $\frac{\mathrm{W}}{\mathrm{K}}$	$T^{\mathrm{H,sh}}$ °C	$T^{\mathrm{sh}}_{\mathrm{max}}$ °C	K_{sun} m^2	$V^{\mathrm{tank}**}$ L	Footage m^2
House	1	4.1	0.5	170	849	3.6	75	70	8	470	369
	2	4.5	0.4	207	616	2.9	75	70	10	341	268
	3	3.4	0.1	208	237	1.6	75	70	10	131	103
	4	3.1	0.1	153	291	2.3	60	55	5	237	186
	5	2.8	0.1	142	399	2.8	60	55	5	325	255
Multi family	6	4.2	0.3	160	718	3.6	65	60	6	467	250
	7	4.9	0.2	182	616	5.3	60	55	5	819	438
	8	9.0	1.3	307	3115	9.6	65	60	12	2026	1084
	9	4.7	0.5	175	1207	5.1	65	60	7	785	420
	10	21.6	3.8	658	9325	20.0	65	60	26	6064	3245
Commercial	11	11.7	0.7	490	2320	2.6	60	55	20	277	1128
	12	25.8	2.1	977	6821	5.2	60	55	39	814	3316
	13	6.1	0.1	284	403	0.8	60	55	11	48	196
	14	7.7	0.3	344	487	0.9	75	70	20	61	247
	15	6.2	0.5	276	789	1.3	75	70	16	98	400

* $R_x = 1/U_x$

** $C^{\mathrm{tank}} = \rho c_p V^{\mathrm{tank}}$ with $\rho = 1$ kg/L, $c_p = 4.18 \cdot 10^3$ J/kg

5 Results

The designs obtained from the MILP are summarized in Figure 8. Note that the PV capacity corresponds for each building to the maximum potential capacity reported in Table 3. For the single-family house and multi-family building, the HP capacity is larger than the EH. There is an apparent economic interest in investing in a HP rather than in an EH because for every unit of electricity sent to the HP, one gets a lot more heat from the HP than from the EH. However, for rare peaks of DHW demand, it might be advantageous to invest in an EH because the specific investment cost is much lower. So for systems that may suffer from large heating peaks, it might be interesting to have a larger electrical capacity. For instance, not-residential buildings have significantly larger EH capacities.

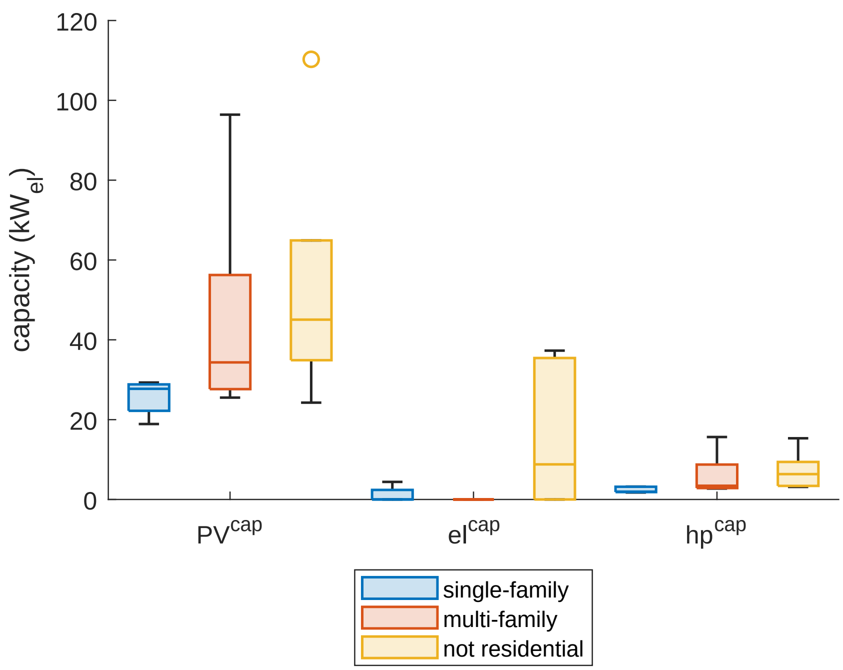

Figure 8: PV, HP, and EH capacity given by the MILP.

The operation is simulated for each typical week and each representative building. An example operation from the MILP and the HCA is represented in Figures 9 and 10, respectively. One may note that the MILP and HCA's operations are very similar. A closer look at Figure 10 highlights that the space heating circuit and the hot water tank's temperature are higher than those of the MILP (Figure 9. This means that the HCA generally uses more heat than the MILP, as shown in Figures 12 for the space heating, and 11 for the DHW.

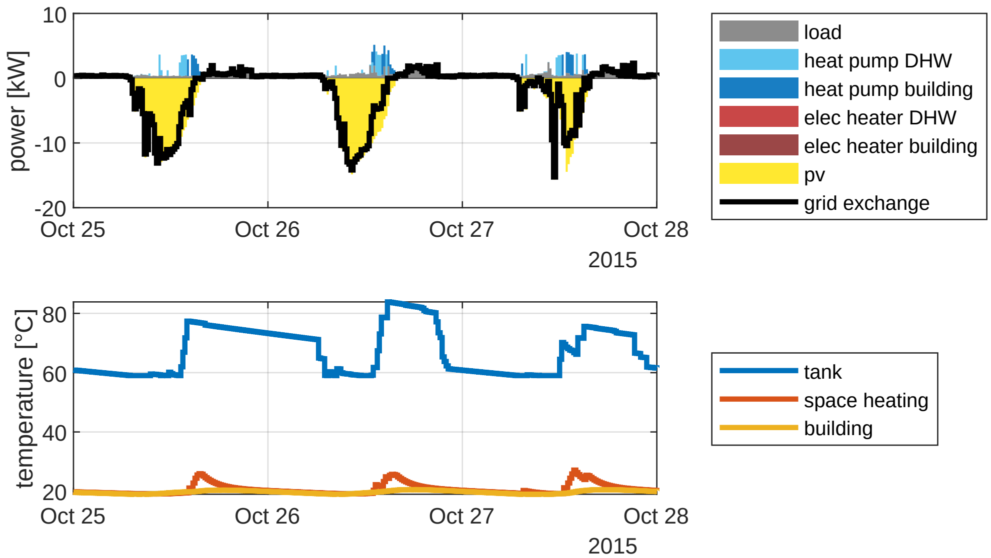

Figure 9: three days operation example resulting from the MILP optimization.

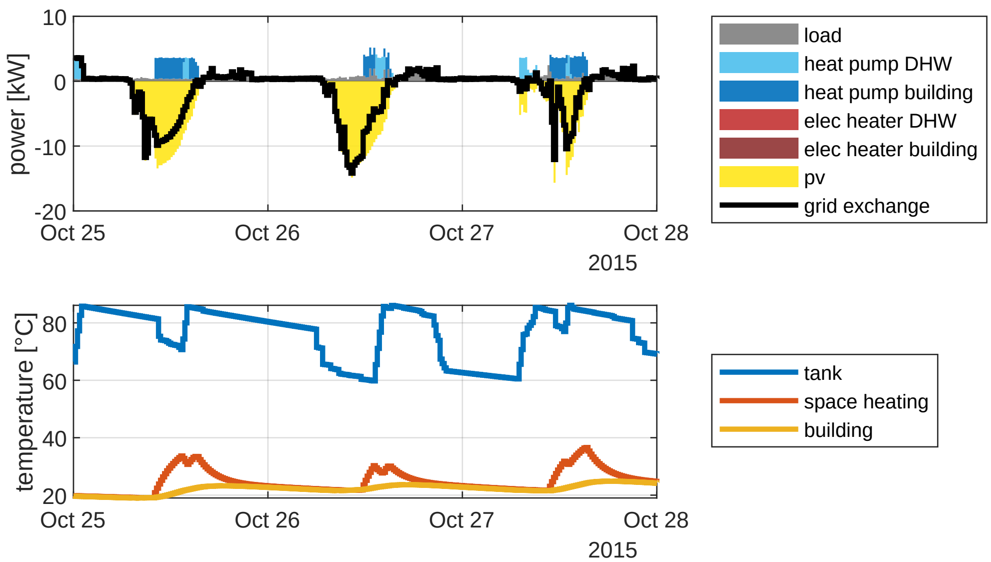

Figure 10: three days operation example resulting from the HCA.

The heat generated from the EH is negligible compared to the heat generated by the HP both for the space heating and DHW as shown in Figures 11 and 12, respectively, even for the non-residential category where larger EH capacities are observed. This enforces the hypothesis that the EH only supports large peaks of heat demand. In Figures 11 and 12, the minimum heat required is also indicated. The difference between the minimum and actual heat generation can be explained by three aspects. First, one should consider the tank heat loss. Second, the objective function is not to minimize the amount of heat consumed, but to minimize the operating cost. Finally, for the HCA only, the non-optimality of the algorithm might induce this larger heat generation. The question arises if the HCA keeps the building warmer.

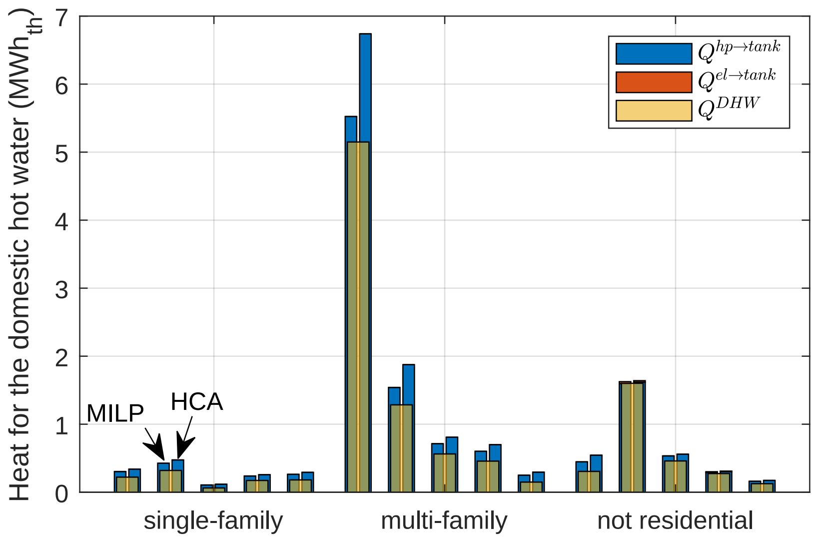

Figure 11: Heat generation for DHW. $Q^{\mathrm{hp}\to\mathrm{tank}}$ is the heat generated by the HP, $Q^{\mathrm{el}\to\mathrm{tank}}$ is the heat generated by the EH (too small to be visible), Q^{DHW} is the DHW heat consumption. The bar of the left corresponds to the MILP, and the one of the right to the HCA.

The mean temperature deviation is reported in Figure 13. Keeping in mind that this is the sum of the absolute temperature deviation from a target comfort temperature, the HCA suffers from a higher temperature deviation. It reaches up to 2.5 °C (absolute value), which can be quite significant from the user's perspective. Nevertheless, these temperature deviations can come from the fact that the external temperature and solar gain can significantly increase the building temperature. Assuming that the MILP provides an optimal building temperature, the temperature deviations, in this case, reach up to 2 °C. This leads to the conclusion that the difference between the HCA and MILP is not so significant. Another aspect that may explain the HCA's higher temperature deviation is that the latter considers the HP's running and switching cost.

The running cost comes from the fact that a HP has a finite lifetime, which can be measured as the total operating hours. The HCA takes it into account and aims to minimize the running time of the HP. The MILP, on his side, does not take into account this aspect in the objective function. This leads, obviously, to a much higher running time for the MILP than for the HCA, as highlighted in Figure 14. It might also explain why the HCA has a higher temperature deviation than the MILP. Similarly, the MILP does not take into account the switching costs.

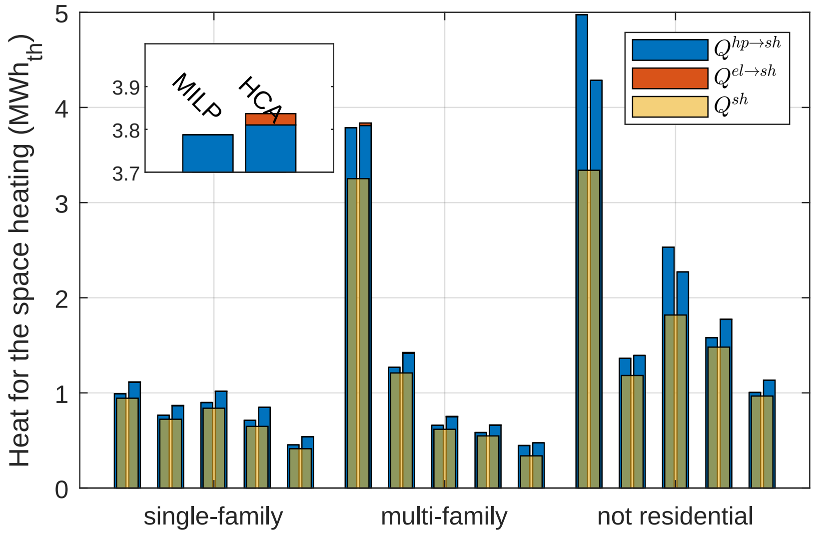

Figure 12: Heat generation for space heating. $Q^{\mathrm{hp}\to\mathrm{sh}}$ is the heat generated by the HP, $Q^{\mathrm{el}\to\mathrm{sh}}$ is the heat generated by the EH (too small to be visible), Q^{sh} is minimum building heat consumption. The bar of the left corresponds to the MILP, and the one of the right to the HCA.

Those come from the fact that switching on and off a HP causes mechanical damage and should be minimized, as in the HCA. Again, the MILP has much higher switching per day than the HCA, as depicted in Figure 15, for the reason just explained. The switching and running costs are virtual costs that help to moderate the HP operation. The real cost of a HP is the investment cost that may be amortized on a shorter lifetime due to more intensive use. This aspect has not been further investigated. The only real, measurable cost is the operating cost. The switching and running cost are not integrated into the MILP objective function because this would require $2T$ additional Boolean decision variables and drastically increase the solving time.

The operating costs for all scenarios (sorted by the ascending MILP $OPEX$ value) are pictured in Figure 16. The blue line, representing the HCA, is very close to the MILP, showing very similar financial results in terms of grid exchange. The total operating cost per building summed across all typical periods is reported in Table 5. The difference between the MILP and the HCA going between 20 cts/day up to 2.55 CHF/day, for an $OPEX$ ranging between -20 CHF/day and 20 CHF/day. The difference can even be in favor of the HCA (the $OPEX$ of the HCA is smaller than the MILP one). Despite the very tiny difference, these surprising results come from the fact that no constraints are applied to the HCA's space heating temperature. It happens that the HCA chooses to over-heat the space heating circuit, self-consuming a little bit more PV energy, while the MILP would stop heating before breaking the temperature upper-bounds.

Finally, the simulation times are reported in Table 6. The MILP problem is solved via

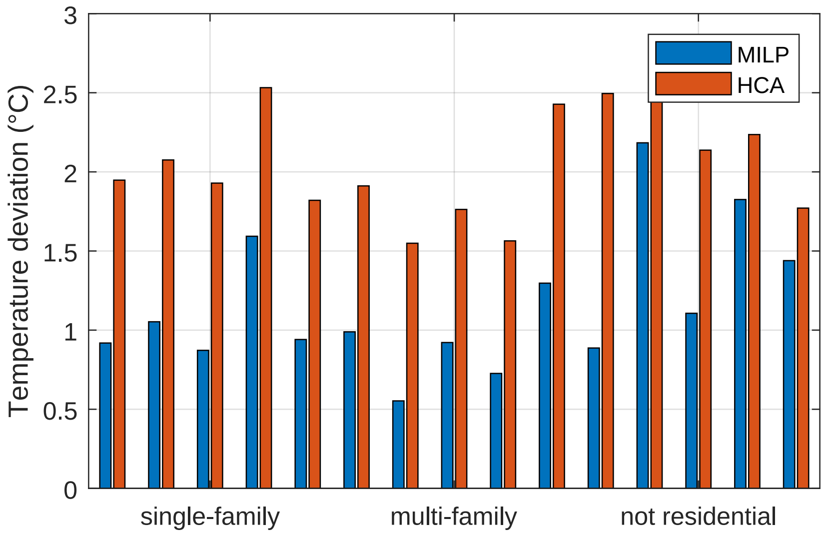

Figure 13: Mean temperature deviation (°C).

GUROBI [32], a very efficient solver, whereas the HCA is a heuristic algorithm. For this reason, the simulation times are much higher for the HCA than for the MILP. However, the HCA can perform the control of a HP in a very short time compared to the length of the period (one week). Moreover, the HCA can cope with all non-linear energy system models, making it suitable for a real implementation. Finally, the MILP requires advanced softwares to solve the optimization problem that are not required by the HCA. Indeed the HCA could be implemented on a simple micro-controller as a state machine.

		MILP	HCA	Δ
single-family	1	-3.02	-2.77	0.26
	2	-4.63	-4.37	0.27
	3	-3.72	-3.55	0.17
	4	-4.69	-4.52	0.17
	5	-5.29	-5.11	0.19
multi-family	6	-7.36	-7.24	0.12
	7	-5.27	-5.07	0.20
	8	-1.16	-0.44	0.71
	9	-2.47	-2.19	0.28
	10	19.53	22.08	2.55
non-residential	11	-9.50	-9.53	-0.03
	12	-22.96	-22.98	-0.02
	13	5.57	5.68	0.12
	14	-5.09	-4.80	0.29
	15	-2.51	-2.31	0.19

Table 5: *OPEX* comparison (CHF/jour)

	min	max	median	mean
MILP	0.07	0.23	0.12	0.13
HCA	15.76	686.35	121.53	172.30

Table 6: Running time (s)

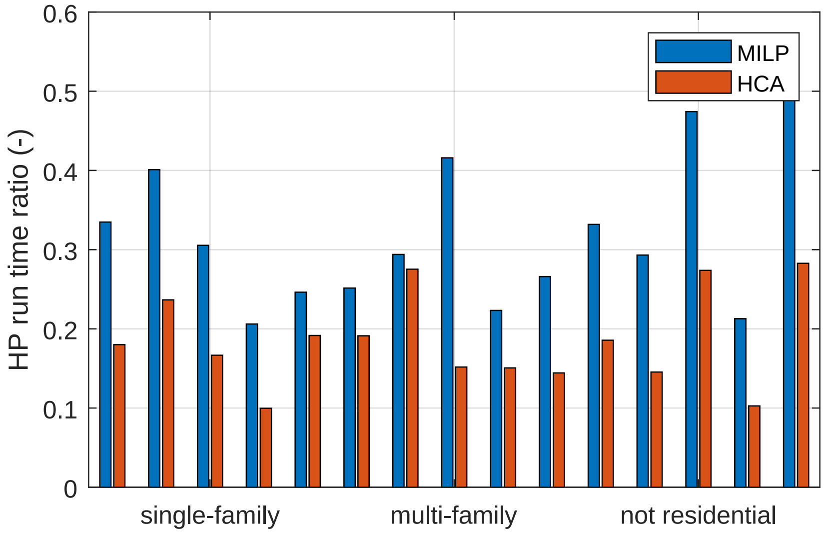

Figure 14: HP running time ratio.

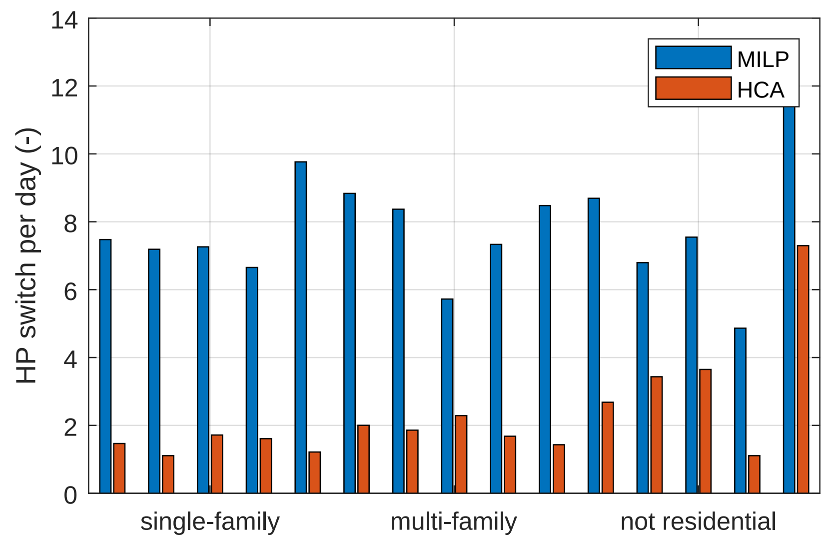

Figure 15: Number of HP switch on per day .

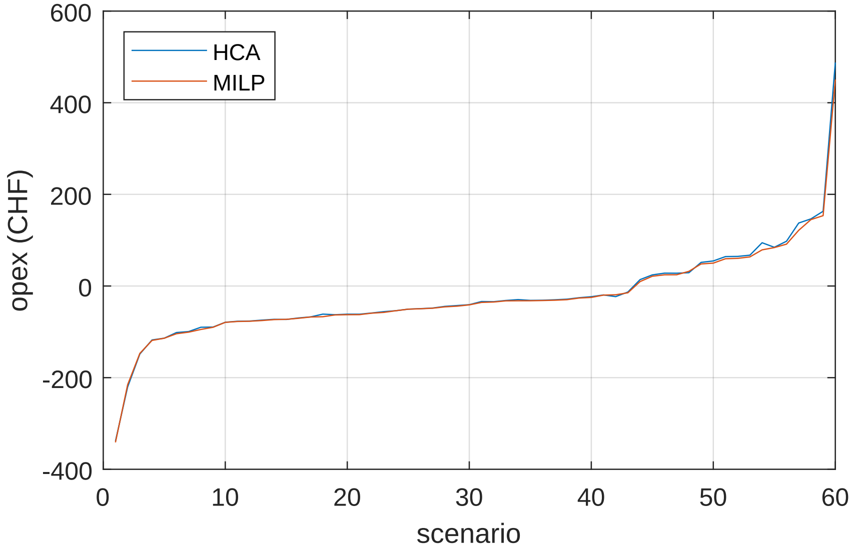

Figure 16: $OPEX$ value for all buildings and scenarios.

6 Conclusions

In this work, we proposed a linear thermal model to obtain the heat pump's (HP) optimal control trajectory by solving the mixed-integer linear problem (MILP). We also presented a novel heuristic control algorithm (HCA) to control a HP and its ancillary electrical heater (EH) in the framework of a PV system in a self-consumption scheme. The HCA is based on an indicator with relates, for all possible actions, the variations of the operating cost, and the variation of the produced heat. The algorithm's primary objective is to keep the temperature state variable in the imposed bounds. This ensures comfort in the building and the appropriate service temperature for the domestic hot water (DHW). The first step is to evaluate the system's behavior and target time windows when temperatures are below the target temperatures and heating is needed. Then, for these time-windows, the algorithm evaluates the value of the indicator and chooses the best set of actions that minimize this indicator.

The HCA is straightforward and an effective control algorithm suitable for implementation in any micro-controller without the need for advanced computing technology. The system behavior's model is versatile, allowing to catch any non-linearities related to the HP behavior under part load or detailed COP calculations. Although it is not implemented yet, it could be possible (at some computation cost) to use a more advanced model for the tank and building temperature (for instance, considering a stratified tank temperature or using a more complex RC model for the building).

Ee used a linear formulation of the problem with the operating cost as the objective function to benchmark this algorithm and solve it using a commercial MILP solver. A set of 15 building models was built to have a representative case study. We also used four typical periods of one week to simulate the HCA's behavior and compare it with the MILP. Under the assumption of a perfect forecast, the HCA's performance is close to the linear problem one. The differences in operating cost are negligible. The temperature deviations can sometimes be significant but stay in the same range as the MILP (recalling that no cooling is allowed, these are mostly due to the external temperature). The HCA, because it includes the HP's running and switching costs, uses the HP more carefully, hence having lower running time and switching than the MILP. This should positively impact the lifetime of the HP in a real application. Despite the HCA's computing time being much larger than the MILP, the HCA has a low computing burden when considering that we simulated one week of operation at 15 min time resolution.

To sum up, the HCA is suitable for a real deployment in a HP and solar controller. The next step would be to test the algorithm on real hardware. Further work should also include the control of an electrochemical battery in the formulation of the indicator.

References

[1] Infras; Prognos; TEP Energy;. Analyse des schweizerischen Energieverbrauchs 2000 - 2019 nach Verwendungszwecken. Technical Report October, Swiss federal office for energy, 2020.

[2] Takashi Shiba, Ryohei Yokoyama, and Koichi Ito. Optimal sizing of a heat pump/thermal storage system based on the linear programming method. *International journal of energy research*, 19(8):665–674, 1995.

[3] Araz Ashouri, Samuel S Fux, Michael J Benz, and Lino Guzzella. Optimal design and operation of building services using mixed-integer linear programming techniques. *Energy*, 59:365–376, 2013.

[4] Hassan Harb, Jan Reinhardt, Rita Streblow, and Dirk Müller. Mip approach for designing heating systems in residential buildings and neighbourhoods. *Journal of Building Performance Simulation*, 9(3):316–330, 2016.

[5] T. Beck, H. Kondziella, G. Huard, and T. Bruckner. Optimal operation, configuration and sizing of generation and storage technologies for residential heat pump systems in the spotlight of self-consumption of photovoltaic electricity. *Applied Energy*, 188:604–619, feb 2017.

[6] C. Verhelst, D. Axehill, C. N. Jones, and L. Helsen. Impact of the cost function in the optimal control formulation for an air-to-water heat pump system. In *8th International Conference on System Simulation in Buildings (SSB), Liege, Belgium*, 2010.

[7] Behrang Alimohammadisagvand, Juha Jokisalo, Simo Kilpeläinen, Mubbashir Ali, and Kai Sirén. Cost-optimal thermal energy storage system for a residential building with heat pump heating and demand response control. *Applied Energy*, 174:275–287, jul 2016.

[8] R. Renaldi, A. Kiprakis, and D. Friedrich. An optimisation framework for thermal energy storage integration in a residential heat pump heating system. *Applied Energy*, 186:520–529, jan 2017.

[9] Georg Angenendt, Sebastian Zurmühlen, Fabian Rücker, Hendrik Axelsen, and Dirk Uwe Sauer. Optimization and operation of integrated homes with photovoltaic battery energy storage systems and power-to-heat coupling. *Energy Conversion and Management: X*, 1(January):100005, 2019.

[10] Evangelos Vrettos, KuanLin Lai, Frauke Oldewurtel, and Göran Andersson. Predictive control of buildings for demand response with dynamic day-ahead and real-time prices. In *European Control Conference (ECC), Zürich, Switzerland*, 2013.

[11] Yang Zhao, Yuehong Lu, Chengchu Yan, and Shengwei Wang. MPC-based optimal scheduling of grid-connected low energy buildings with thermal energy storages. *Energy and Buildings*, 86:415–426, jan 2015.

[12] Sebastian Kuboth, Florian Heberle, Theresa Weith, Matthias Welzl, Andreas König-Haagen, and Dieter Brüggemann. Experimental short-term investigation of model predictive heat pump control in residential buildings. *Energy and Buildings*, 204, 2019.

[13] Hector Bastida, Carlos E. Ugalde-Loo, Muditha Abeysekera, Meysam Qadrdan, Jianzhong Wu, and Nick Jenkins. Dynamic Modelling and Control of Thermal Energy Storage. *Energy Procedia*, 158:2890–2895, feb 2019.

[14] Amjad Anvari-Moghaddam, Hassan Monsef, and Ashkan Rahimi-Kian. Cost-effective and comfort-aware residential energy management under different pricing schemes and weather conditions. *Energy and Buildings*, 86:782–793, jan 2015.

[15] Yannick Riesen, Christophe Ballif, and Nicolas Wyrsch. Control algorithm for a residential photovoltaic system with storage. *Applied Energy*, 202:78–87, sep 2017.

[16] Cristian Sánchez, Lionel Bloch, Jordan Holweger, Christophe Ballif, and Nicolas Wyrsch. Optimised Heat Pump Management for Increasing Photovoltaic Penetration into the Electricity Grid. *Energies*, 12(8):1571, apr 2019.

[17] Maximilian Schulz, Thomas Kemmler, Julia Kumm, Kai Hufendiek, and Bernd Thomas. A more realistic heat pump control approach by application of an integrated two-part control. *Energies*, 13(11), 2020.

[18] Zahra Rahimpour, Gregor Verbič, and Archie C. Chapman. Actor-critic learning for optimal building energy management with phase change materials. *Electric Power Systems Research*, 188:106543, nov 2020.

[19] Bing Yan, Marialaura Di Somma, Giorgio Graditi, and Peter B. Luh. Markovian-based stochastic operation optimization of multiple distributed energy systems with renewables in a local energy community. *Electric Power Systems Research*, 186(April):106364, 2020.

[20] Lionel Bloch, Jordan Holweger, Christophe Ballif, and Nicolas Wyrsch. Impact of advanced electricity tariff structures on the optimal design, operation and profitability of a grid-connected PV system with energy storage. *Energy Informatics*, 2(1):16, 2019.

[21] SIA. *Donnees d'utilisation des locaux pour l'energie et les installations du batiment*, volume 4. Zurich, 2015.

[22] Leonard Kaufman and Peter J Rousseeuw. *Finding groups in data: an introduction to cluster analysis*, volume 344. John Wiley & Sons, 2009.

[23] Lionel Perret, Joëlle Fahrni, Nicolas Wyrsch, Yannick Riesen, Stefano Puddu, Sylvain Weber, and Diana Pfacheco Barzallo. FLEXI Determining the flexibilization potential of the electricity demand. 2015.

[24] Lionel Perret, Yves Chevillat, Nicolas Wyrsch, Lionel Bloch, Jordan Holweger, Sylvain Weber, and Martin Péclat. Flexi 2 Déterminer le potentiel de flexibilisation de la demande d ' électricité des ménages. Technical report, Fedral office for energy, 2019.

[25] M. Roux, M. Apperley, and M.J. Booysen. Comfort, peak load and energy: Centralised control of water heaters for demand-driven prioritisation. *Energy for Sustainable Development*, 44:78–86, jun 2018.

[26] M.J. Booysen, J.A.A. Engelbrecht, M.J. Ritchie, M. Apperley, and A.H. Cloete. How much energy can optimal control of domestic water heating save? *Energy for Sustainable Development*, 51:73–85, aug 2019.

[27] Leander Kotzur, Lars Nolting, Maximilian Hoffmann, Theresa Groß, and Andreas Smolenko. A modeler ' s guide to handle complexity in energy system optimization. 2020.

[28] Maximilian Hoffmann, Leander Kotzur, Detlef Stolten, and Martin Robinius. A review on time series aggregation methods for energy system models. *Energies*, 13(3), 2020.

[29] Umit Cetinkaya, Ezgi Avci, and Ramazan Bayindir. Time Series Clustering Analysis of Energy Consumption Data. pages 409–413, 2020.

[30] David Fischer, Karen Byskov Lindberg, Hatef Madani, and Christof Wittwer. Impact of PV and variable prices on optimal system sizing for heat pumps and thermal storage. *Energy and Buildings*, 128:723–733, 2016.

[31] Householdquotes. Electric Combi Boilers: A Cost-Effective Way To Heat Small Homes?, 2020.

[32] LLC Gurobi Optimization. Gurobi optimizer reference manual, 2020.